The effect of reflow profile on SnPb and SnAgCu solder joint shear strength

Jianbiao Pan
California Polytechnic State University, San Luis Obispo, California, USA

Brian J. Toleno
Henkel Technologies, Irvine, California, USA, and

Tzu-Chien Chou and Wesley J. Dee
California Polytechnic State University, San Luis Obispo, California, USA

Abstract

Purpose – The purpose of this work is to study the effect of the reflow peak temperature and time above liquidus on both SnPb and SnAgCu solder joint shear strength.

Design/methodology/approach – Nine reflow profiles for Sn3.0Ag0.5Cu and nine reflow profiles for Sn37Pb have been developed with three levels of peak temperature (230°C, 240°C, and 250°C for Sn3.0Ag0.5Cu; and 195°C, 205°C, and 215°C for Sn37Pb) and three levels of time above solder liquidus temperature (30, 60, and 90 s). The shear force data of four different sizes of chip resistors (1206, 0805, 0603, and 0402) are compared across the different profiles. The shear forces for the resistors were measured after assembly. The fracture interfaces were inspected using scanning electron microscopy with energy dispersive spectroscopy in order to determine the failure mode and failure surface morphology.

Findings – The results show that the effects of the peak temperature and the time above solder liquidus temperature are not consistent between different component sizes and between Sn37Pb and Sn3.0Ag0.5Cu solder. The shear force of SnPb solder joints is higher than that of Sn3.0Ag0.5Cu solder joints because the wetting of SnPb is better than that of SnAgCu.

Research limitations/implications – This study finds that fracture occurred partially in the termination metallization and partially in the bulk solder joint. To eliminate the effect of the termination metallization, future research is recommended to conduct the same study on solder joints without component attachment.

Practical implications – The shear strength of both SnPb and SnAgCu solder joints is equal to or higher than that of the termination metallization for the components tested.

Originality/value – Fracture was observed to occur partially in the termination metallization (Ag layer) and partially in the bulk solder joint. Therefore, it is essential to inspect the fracture interfaces when comparing solder joint shear strength.

Keywords Fracture, Shear strength, Soldering

Introduction

The increasing concern there may be a health risk associated with lead (Pb) containing solder alloys has pushed the electronics industry toward lead-free assembly. Legislation banning the use of lead is only one of the driving forces. From the business point of view, lead-free electronic products (perceived as being green products) are also a market trend.

Among the many lead-free solder alloys developed, SnAgCu lead-free solder alloys are considered by the electronics industry to be the best alternative to eutectic tin-lead solder (Handwerker, 2005; Nurmi *et al.*, 2005). The alloy has also been recommended by several industry consortiums including the Inter-National Electronics Manufacturing Initiative (iNEMI), an EU consortium known as IDEALS (improved design life and environmentally aware manufacturing of electronic assemblies by lead-free soldering), and the Japan Electronics and Information Technology Industries Association (JEITA). One of the major differences between SnPb and SnAgCu lead-free solders is that SnAgCu solders require a higher reflow temperature than eutectic SnPb. The melting point of SnAg3.8Cu0.7 is 219°C, and that of SnAg3.0Cu0.5 is 217°C, compared with eutectic SnPb solder, which has a melting point of 183°C. This higher melting temperature not only requires a new reflow profile, but also increases component reliability concerns.

An effective transition from SnPb soldering to lead-free soldering requires key implementation issues to be addressed

This work was sponsored by the Department of the Navy, Office of Naval Research, under Award Number N00014-05-1-0855. The authors would like to thank Henkel Technologies for providing a stencil, solder paste, shear testing, and SEM sample preparation. The authors also want to thank Charlson Bernal and Roger Jay for SEM analysis, and Jasbir Bath, Dennis Willie, and Kim Hyland of Solectron Corp. for technical support. Special thanks to Flextronics International, DEK, Siemens, and Heller Industries for sponsoring the surface mount assembly line at Cal Poly, where the boards were assembled.

in the electronics industry. One of the critical issues is the effect of reflow profile on lead-free solder joint reliability, since the reflow profile would influence wetting and the microstructure of the solder joint. Solder pastes require an adequate reflow temperature to melt, wet, and interact with the copper pad or other board metallization and component metallization to form the solder joint. Intermetallic layers, which are an essential feature of the bond, will form during the reflow and cooling processes. A suitable reflow profile is therefore essential to form a good solder joint.

Research studies show that the peak temperature and time above liquidus (TAL) during the reflow process are the most critical parameters impacting solder joint reliability (Arra *et al.*, 2002; Salam *et al.*, 2004). For SnAgCu reflow soldering, it is commonly accepted that a minimum peak temperature of 230°C is necessary to achieve acceptable solder joints. The maximum temperature, on the other hand, depends on the board size, board thickness, component configuration, material thermal mass, oven capability, etc. These factors result in different temperature deltas across the board, which can sometimes be as high as 20-25°C. Moreover, larger components and thicker boards lead to a higher temperature delta across the board, thus demanding a longer TAL in order to achieve sufficiently uniform peak temperatures across the entire printed wiring board (PWB).

Good solder joint strength mainly depends on two factors: the bulk microstructure of the solder joint and the intermetallic layer. The microstructure of SnAgCu solder joints is different from that of SnPb joints, due to the presence of Cu_6Sn_5 and Ag_3Cu intermetallic compounds (IMC) in the bulk solder (Salam *et al.*, 2004). Note that in a SnPb solder joint, Cu_6Sn_5 is present only at the interface between SnPb solder and the Cu pad. Generally speaking, the faster cooling rate would result in a finer gain size, which would strengthen the solder joint.

The intermetallic layer thickness is another factor that would impact solder joint strength. The intermetallic layer is a critical part of a solder joint, because it facilitates bonding between the solder and the substrate. However, too thick an intermetallic layer has an adverse effect, because it is generally the most brittle part of the solder joint. Compared to lead-based solders, SnAgCu solders require a higher reflow temperature, which leads to accelerate diffusion rates. With a higher reflow temperature and a longer TAL, more substrate metallization is dissolved and more intermetallics are formed (Arra *et al.*, 2002). Solder joint strength may be affected by both lack of intermetallic formation as well as excess intermetallics. Hence, an optimum combination of peak temperature and TAL is important to achieve a good solder joint.

The purpose of this experiment is to study the effect of the reflow peak temperature and TAL on solder joint shear strength. Nine reflow profiles for Sn3.0Ag0.5Cu (SAC305) and nine reflow profiles for Sn37Pb have been developed with three levels of peak temperature (230°C, 240°C, and 250°C for SAC 305; and 195°C, 205°C, and 215°C for SnPb) and three levels of time above solder liquidus temperature (30, 60, and 90 s). The shear strength data for four different sizes of chip resistors (1206, 0805, 0603, and 0402) are compared across the different profiles. Note that 1206 means a component with a nominal length of 0.12 in. (3.0 mm) and a nominal width of 0.06 in. (1.5 mm). The shear forces for the resistors were measured after assembly. The fracture interfaces were inspected using scanning electron microscopy (SEM) in order to determine the failure mode and failure surface morphology.

Experimental design and procedures

A 3^2 factorial design with three replications was selected for the experiment. The peak temperature and TAL are the two input factors and each factor has three levels: peak temperature at 230°C, 240°C, and 250°C for SAC305 and 195°C, 205°C, and 215°C for SnPb, and TAL at 30, 60, 90 s, for both, as shown in Table I. Note that the peak temperatures selected are 12°C, 22°C, and 32°C above SnPb or SnAgCu solder liquidus temperatures. Four different sizes of pure tin plated chip resistors, 1206, 0805, 0603, and 0402 were used in this experiment. The solder paste, components and the board metallization used in the experiment are shown in Table II.

The test vehicle designed is shown in Figure 1. It is a single layer board with a thickness of 1.57 mm (62 mils) and size of 98.4 × 135.5 mm (3.875 × 5.375 in.). The board material is FR-4 and there are 14 components per size per board.

Table I Experimental variable matrix

Peak temperature (°C)	SAC305	230	240	250
	SnPb	195	205	215
TAL (s)		30	60	90

Table II Solder pastes, components, and board metallizations in the experiment

Solder paste	Components and metallization	Board metallization
SAC305, type 3 powder, no-clean flux	1206, 0805, 0603, 0402 all 100 per cent Sn finish	OSP over Cu pad
Sn63Pb37, type 3 powder, no-clean flux	1206, 0805, 0603, 0402 all 100 per cent Sn finish	HASL SnPb over Cu pad

Figure 1 Test vehicle

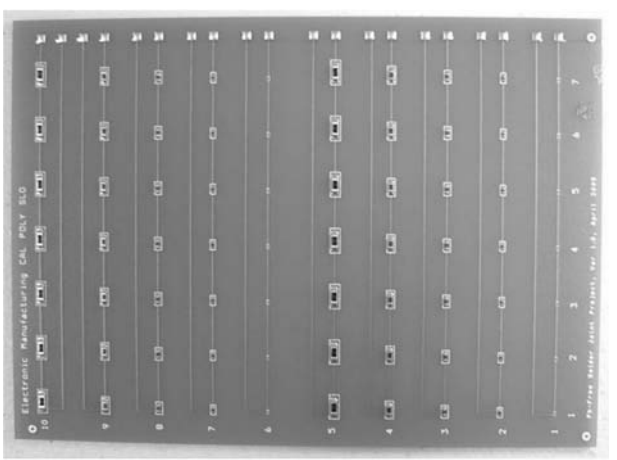

The solder paste printing process was performed using a DEK265 Horizon series stencil printer. A 100 μm (4 mil) thick laser-cut electro-polished stencil was used. The printing quality was inspected using a microscope. A Heller 1500 convection oven with five heating zones and one cooling zone was used for solder reflow. The 18 reflow profiles were developed using three thermocouples attached to the test vehicle at the diagonal corners of the board and the centre. A linear ramp-up method or ramp-to-spike method was used for developing the reflow profiles. For detailed information on the ramp-to-spike method please refer to Bentzen (2000), Suraski (2000), Lau *et al.* (2003) and Salam *et al.* (2004). Figure 2 shows a sample lead-free reflow profile.

Since, it is a 3^2 factorial design with three replications, 27 boards were assembled using SnPb paste and 27 boards were assembled using SAC305 paste. The assembly was conducted over two days, the SnPb boards were assembled in one day and SAC305 boards were assembled the next day. The assembly sequence during each day was randomized to minimize any nuisance factors such as room temperature, humidity, and other conditions. To be consistent, the process parameters for the stencil printing and pick and place were the same. The only variable is the reflow profile. When moving from one profile to another, the oven settings were changed and allowed to get to temperature (i.e. waiting for the green light), and then allowed to stabilize for at least 5 min.

All boards were visually inspected after stencil printing, after pick and place, and after reflow. The only difference between the SnPb solder joints and SAC305 solder joints after reflow was that the SnPb joints looked shiny and SAC305 joints looked dull. Figure 3 shows sample microscopy images after printing, after component placement, and after reflow.

Shear testing was performed using a Dage series 4000 shear tester. Table III shows the parameters used for the shear tests. Note that the shear force depends on shear speed (Newman, 2005). Each board was cut into two identical pieces. The first half of the board was used for these time zero measurements (right after assembly) and the other half is being used for air-to-air thermal shock testing, for which the results will be published later. For each half sample, six components of each component size (e.g. 0603, 1206, etc.) on each board were sheared, with one component left for SEM analysis. Therefore, 1,292 data (6 components × 3 boards × 4 components sizes × 18 reflow profiles) were collected. Note that the sample size for each component type and reflow profile is 18 (6 components per board × 3 boards). The peak shear force and the failure mode were recorded.

It should be noted that only two failure modes were observed during the shear testing. They are fracture at the solder joint and component failure. For most of the samples the fracture mode was at the solder joint interface. In the data analysis described in the next section, the shear force of samples where the component failed was not considered. Only the shear force data where solder joint fracture occurred were analyzed.

Statistical data analysis

The solder joint shear force data were analyzed using analysis of variance (ANOVA). First, the validity of three assumptions (normally, independently, and constant variance of the residues) of ANOVA was checked (Montgomery, 1997). As shown in Figures 4 and 5, the residual vs predicted shear force plots show that the residual variances are not constant. In order to make the ANOVA analysis valid, a transformation is necessary. It was found the square root transformation was appropriate in this case.

Figure 2 A sample lead-free reflow profile

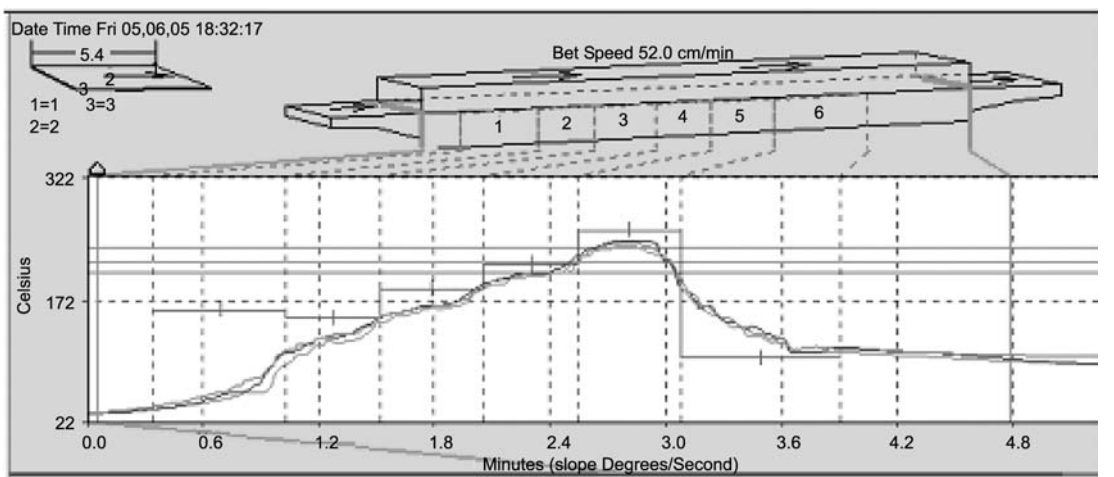

	Peak	Max Rising Slope	Max Falling Slope	Rising Time Between 204/217	Total Time Above 217	Total Time Above 235	Pointer 0.1	Slope 5.52	Pointer 5.6
1.1	237.5	4.62	–6.58	5.32	28.68	7.65	33.1	0.16	87.0
2.2	243.0	5.05	–7.37	7.63	32.14	21.30	34.8	0.13	77.0
3.3	241.0	4.30	–6.31	5.61	30.97	15.83	34.8	0.20	
TC Mean	240.5	4.66	–6.75	6.19	30.59	14.93	34.2	0.16	82.0

Figure 3 Microscope images: (a) after stencil printing; (b) after component being placed; and (c) after reflow

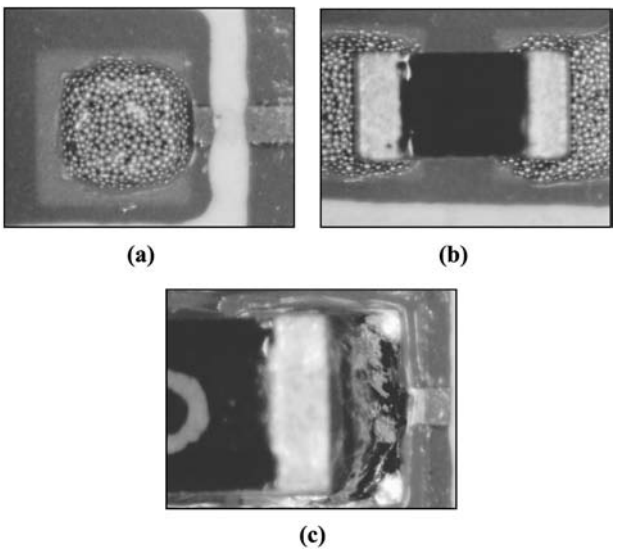

Table III Shear tester parameters

Parameters	Settings
Range	20 kg
Test speed	200 μm/s
Test load	0.5 kg
Land speed	475 μm/s
Shear height	125 μm
Over travel	250 μm

Figure 4 Plot of residuals versus predicted shear force for the SnPb joints

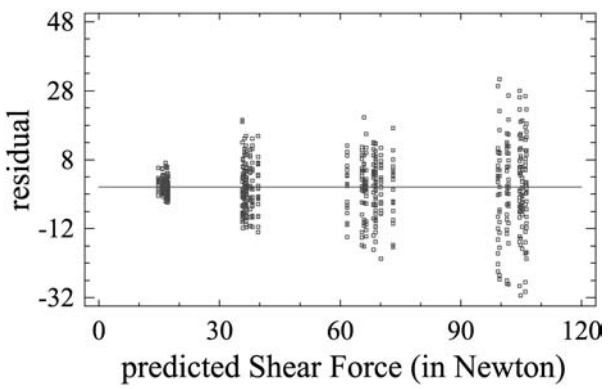

The ANOVA table for the square root of the SAC305 shear force (shear force after transformation) is shown in Table IV. The *P*-value of less than 0.05 indicates that the factor has a statistically significant effect at the 95 per cent confidence level. Table IV shows that the component size, reflow peak temperature and TAL have a statistically significant effect on the shear force. It is intuitive that component size has a significant effect on the solder joint shear force since big components have larger contact areas. Figure 6 shows that the peak temperature of 250°C results in the highest shear force, while there is no significant difference in shear force between the peak temperature of 230°C and 240°C. Figure 7 shows that a TAL of 30 s results in the highest shear force, while there is no significant difference in shear force between the TAL of 60 and 90 s.

The ANOVA table for the square root of the SnPb shear force (shear force after transformation) is shown in Table V. It shows that only the component size and the peak temperature have a statistically significant effect on the shear force. TAL does not

Figure 5 Plot of residuals versus predicted shear force for the SAC305 joints

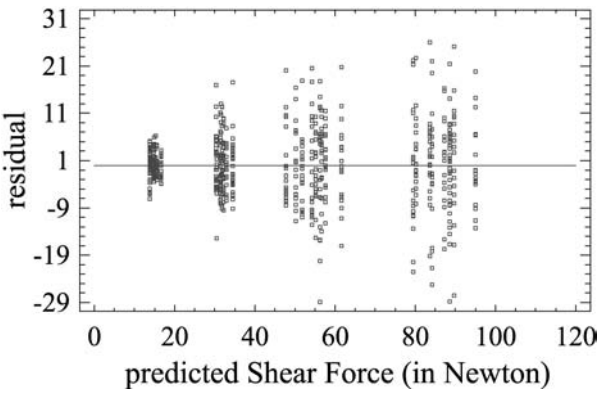

Table IV ANOVA for the square root of the SAC305 shear force

Source	Sum of squares	Df	Mean square	*F*-ratio	*P*-value
Main effects					
A: component size	2,625.72	3	875.2	3,381.98	0.0000
B: peak temp	9.29	2	4.64	17.94	0.0000
C: TAL	8.78	2	4.39	16.96	0.0000
Interactions					
AB	2.37	6	0.39	1.53	0.1670
AC	4.20	6	0.70	2.70	0.0134
BC	1.56	4	0.39	1.51	0.1962
Residual	161.5	624	0.259		
Total (corrected)	2,813.4	647			

Figure 6 Effect of peak temperature on SAC305 solder joint shear force

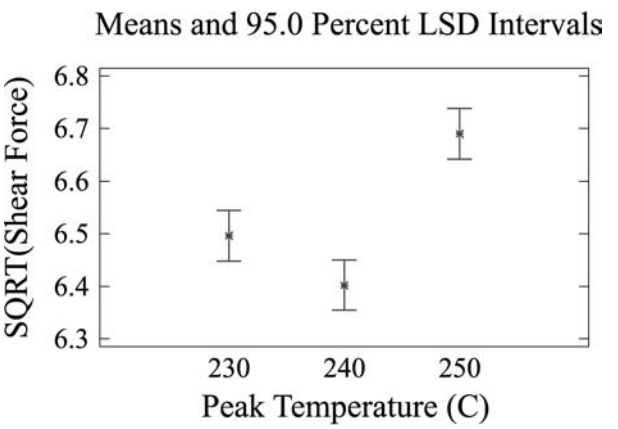

Figure 7 Effect of TAL on SAC305 solder joint shear force

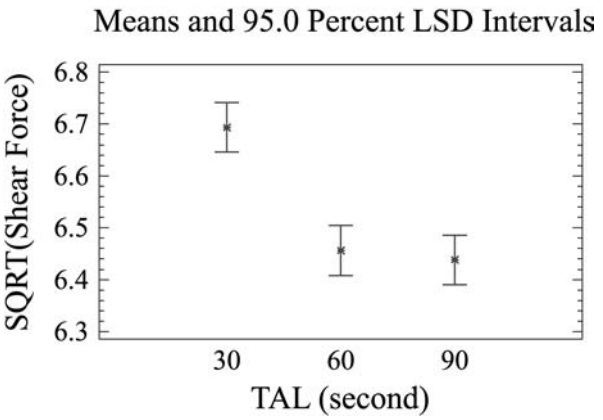

Table V ANOVA for the square root of the SnPb shear force

Source	Sum of squares	Df	Mean square	*F*-ratio	*P*-value
Main effects					
A: component size	3,383.4	3	1,127.8	4,011.01	0.0000
B: peak temp	1.85	2	0.93	3.29	0.0377
C: TAL	0.51	2	0.25	0.90	0.4052
Interactions					
AB	3.43	6	2.03	2.03	0.0596
AC	3.51	6	2.08	2.08	0.0533
BC	1.32	4	1.18	1.18	0.3186
Residual	175.45	624	0.28		
Total (corrected)	3,569.48	647			

have a statistically significant effect on the SnPb solder joint shear force. Figure 8 shows that the peak temperature of 215°C results in a slightly higher shear force, while there is no significant difference in shear force between the peak temperatures of 195°C and 205°C.

In this study, ANOVA for each component size was conducted as well. The effects of the peak temperature and the TAL are summarized in Table VI. The results are confusing because the effect of the peak temperature and the TAL are different for different component sizes. To understand the experimental results, failure analysis using SEM with energy dispersive spectroscopy was performed and the findings will be presented in the next section.

Figure 8 Effect of peak temperature on SnPb solder joint shear force

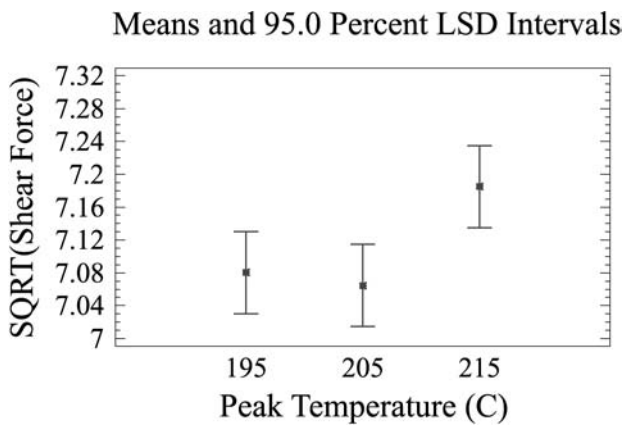

Table VII summarizes the mean shear force for different component sizes. It shows that the shear force for SnPb solder joints is higher than that of SAC305 solder joints for the same component size. The shear force is the product of the shear strength of the joint and the joint contact area (or the solder wetting area). The normalized shear force or shear strength is shown in Table VII as well as in Figure 9. The normalized shear force or shear strength is 69 MPa for SnPb solder joints and 59 MPa for SAC305 solder joints. Note that the contact area is assumed to be the metallization area of the bottom of the chip component. The joint contact area of the fillet (i.e. the component sides) is not considered. The published shear strength of Sn37Pb solder alloy is 45.5 MPa in Table 1.14 of the NIST solder properties database and the shear strength of Sn3.8Ag0.7Cu alloy is 63.8 MPa in Table 1.17 of the NIST solder properties database (Siewert *et al.*, 2002). It is reasonable to assume that the shear strength of Sn3.8Ag0.7Cu is similar to that of Sn3.0Ag0.5Cu. The difference in solder shear strength between this study and the NIST solder database is believed to be due to the different microstructure of the solder joint resulting from the reflow process. The shear strength data from bulk solder specimens may not represent the behaviour of actual solder joints where the scale of the microstructure may have an effect (Rodgers *et al.*, 2005). In the published literature, conflicting results for the SnPb solder joint shear force and SnAgCu solder joint shear force have been reported. For example, Oliver *et al.* (2000) reported that the shear force of Sn37Pb was unexpectedly higher than that of lead-free solder joints before thermal aging while Sampathkumar *et al.* (2005) reported that the shear force of SnAgCu solder joints is higher than that of SnPb solder joints.

Another possible reason for the higher shear force of SnPb than that of SnAgCu could be that the actual joint contact area of SnPb is larger than that of SnAgCu. This correlates with the known wetting differences between SnAgCu and SnPb solders. The fracture area of the solder joints was examined using optical microscopy, for which the results will be presented in the next section.

Optical inspection and SEM analysis

To explain why the shear force of SnPb solder joints is higher than that of SAC305 solder joints, an optical microscope was used to examine the solder joint fracture areas. Figures 10 and 11 show typical fracture areas of SAC305 solder joints and SnPb solder joints. Note that the TAL and the temperature difference between the peak temperature and the liquidus temperature are the same for both SnPb and SAC305 solder joints in both figures. Figures 10 and 11 clearly show that the fracture areas of the SnPb joint is larger than that of the SAC305 joint. Here the joint contact area in fillet (side) is not considered.

To understand why the effects of the peak temperature and the TAL are not consistent for different component sizes and for SnPb and SAC305 solder joints, SEM analysis was conducted. Figures 12 and 13 show the SEM pictures of SnPb joint fracture area and SAC305 joint fracture area. As expected, Sn and Pb were found in SnPb joint fracture and Sn, Ag, and Cu were found in the SnAgCu joint fracture area. But it is interesting to note that a large Ag layer was also detected in both SnPb and SnAgCu fracture areas. The area

Table VI Summary of ANOVA results for each component size

		SAC305	SnPb
1206	Peak temperature	Significant	Not significant (*P*-value = 0.6)
	TAL	Significant	Not significant (*P*-value = 0.1)
0805	Peak temperature	Significant	Significant
	TAL	Significant	Significant
0603	Peak temperature	Not significant (*P*-value = 0.07)	Not significant (*P*-value = 0.27)
	TAL	Not significant (*P*-value = 0.2)	Not significant (*P*-value = 0.66)
0402	Peak temperature	Not significant (*P*-value = 0.1)	Not significant (*P*-value = 0.46)
	TAL	Not significant (*P*-value = 0.06)	Not significant (*P*-value = 0.55)

Note: Significance at 95 per cent confidence level

Table VII Comparison of shear force between SnPb solder joints and SAC305 solder joints

	Average shear force of 324 solder joints (*N*)			Normalized shear strength (MPa)	
Component size	**SAC305**	**SnPb**	**Theoretical contact area (mm^2)**	**SAC305**	**SnPb**
0402	14.84	16.43	0.25	59.35	65.74
0603	32.17	36.95	0.48	67.03	76.97
0805	54.59	67.62	0.96	56.86	70.44
1206	86.30	103.25	1.6	53.94	64.53

Figure 9 Average shear force and shear strength of solder joints

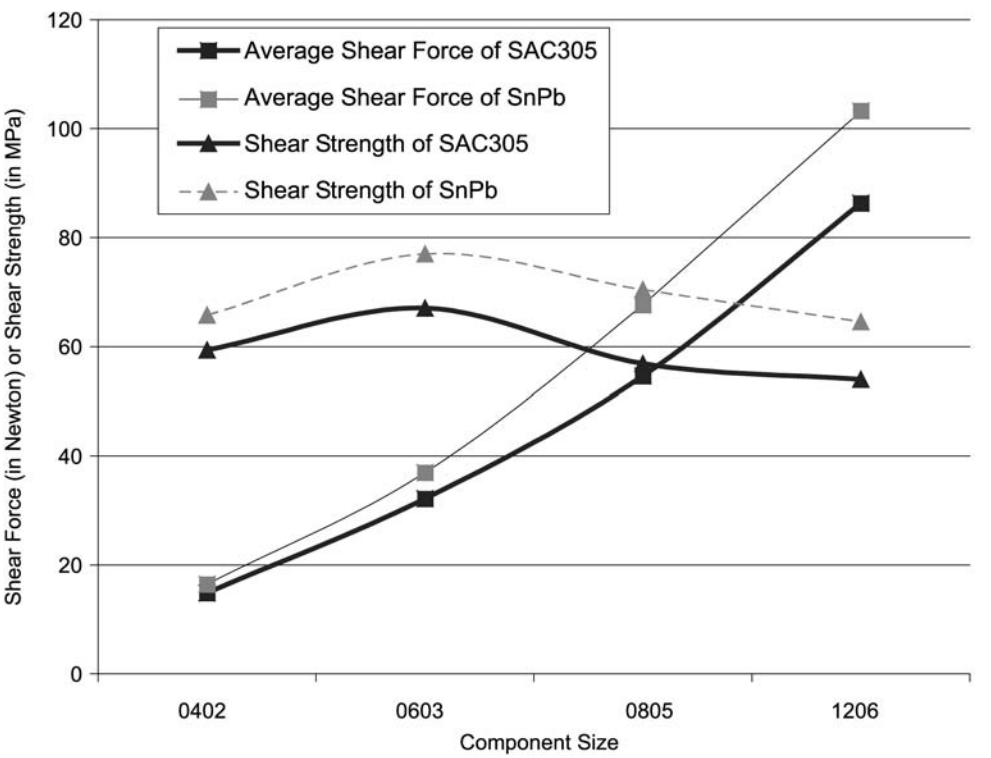

of this Ag layer is larger than or similar to that of SnPb or SnAgCu. But the proportion of the Ag area in the total fracture area varies from one joint to another.

The typical termination structure of lead-free chip resistors is shown in Figure 14. Since, Ag presents in the fracture area, it means that the fracture happens partially in the termination metallization and partially in the bulk solder joints. Since, the proportion of the shear area in the termination metallization varied between different components and component sizes, this may explain why the effects of the peak temperature and the TAL are not consistent for different component sizes and for the SnPb and SAC305 joints.

Figure 10 Fracture area of a SAC305 joint reflowed at 230°C for 30 s

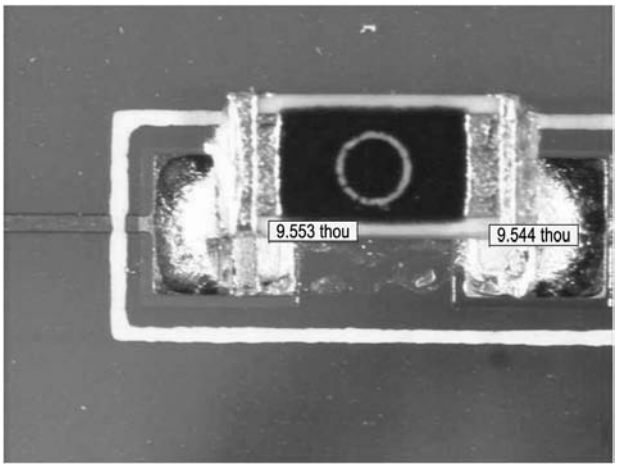

Figure 11 Fracture area of a SnPb joint reflowed at 195°C for 30 s

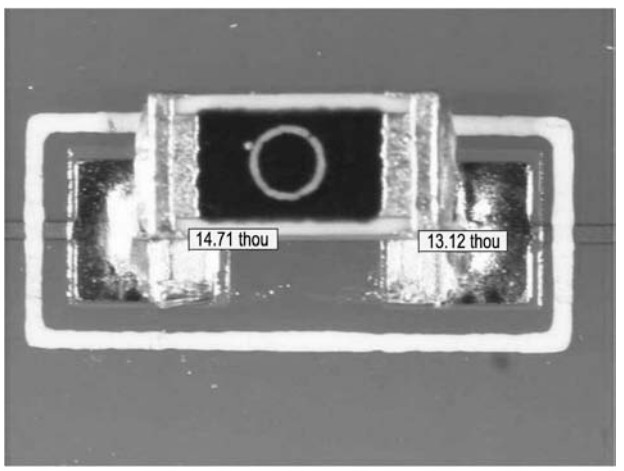

Figure 12 Fracture area of SnPb joint reflowed at 215°C for 90 s

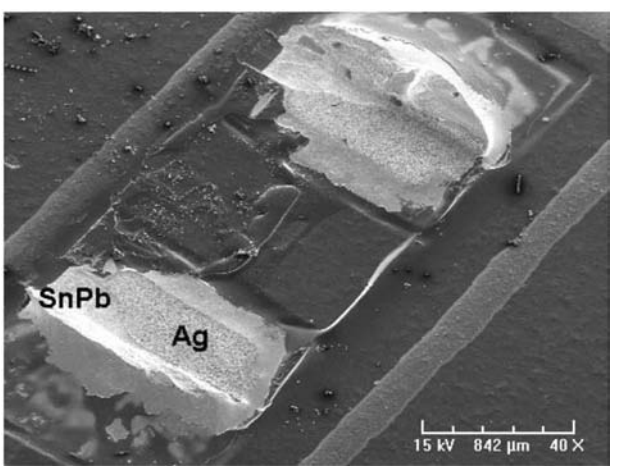

Cross-sections of a SnPb solder joint and a SAC305 solder joint at the highest peak temperature setting (215°C for SnPb solder and 250°C for SAC305 solder) and the longer TAL (90 s) are shown in Figures 15 and 16, respectively.

Figure 13 Fracture area of SAC305 joint reflowed at 250°C for 90 s

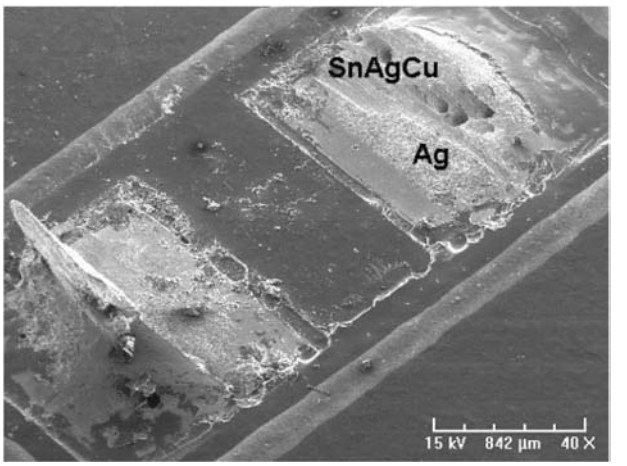

Figure 14 Typical termination structure of a lead free chip resistor

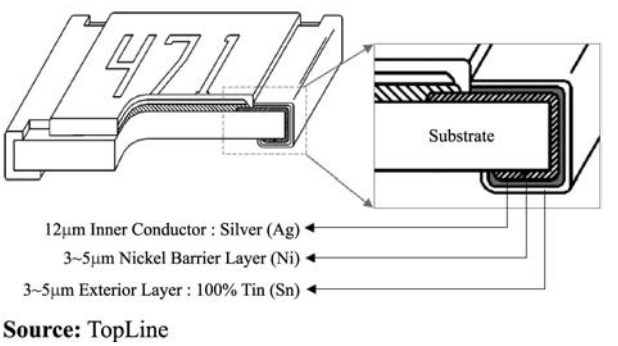

Source: TopLine

Figure 15 Cross-section of a SnPb solder joint reflowed at 215°C for 90 s

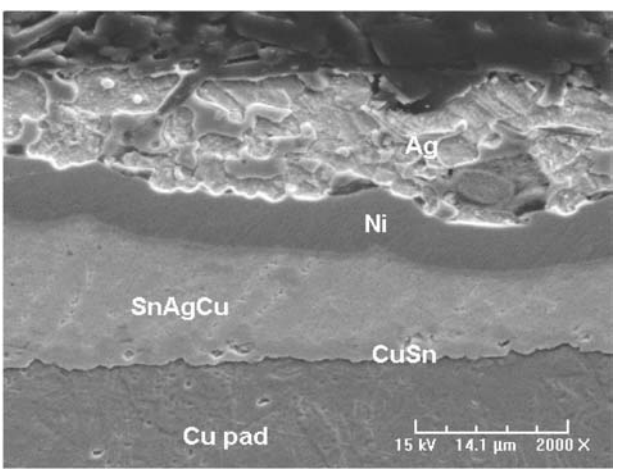

The component size in both figures is 0603. They show that the Sn layer in the chip component metallization was dissolved in the bulk SnPb or SnAgCu joints; a CuSn intermetallic compound (IMC) layer was formed between the bulk solder and the Cu pad and a thin NiSn IMC layer was formed between the bulk solder and the component. They also show the Ag layer

Figure 16 Cross-section of a SAC305 solder joint reflowed at 250°C for 90 s

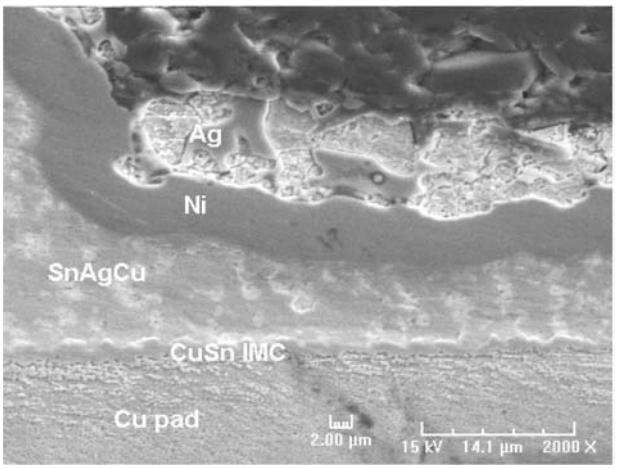

above the Ni layer. The fractures occured partially in the Ag layer and partially in the bulk solder joint, which implies that the shear strength of solder joint is higher than or equal to that of the component metallization.

Conclusions

The following conclusion can be drawn from this study:

- The effects of the peak temp and the TAL are not consistent for different component sizes and for SnPb and SAC305 solder joints. For SAC305 solder joints, higher peak temperature and shorter TAL lead to higher shear strength of solder joints.
- Fracture was observed to occur partially in the termination metallization (Ag layer) and partially in the bulk solder joints for all solder joints inspected. Therefore, it is essential to inspect the fracture interfaces when comparing solder joint shear strength.
- Fracture partially in the Ag layer implies that the shear strength of solder joints is higher than or equal to that of the component metallization.
- The shear force of SnPb solder joints is higher than that of the SAC305 solder joints because the wetting is better, and therefore the joint area is larger, for SnPb than for SnAgCu.

References

Arra, M., Shangguan, D., Ristolainen, E. and Lepisto, T. (2002), "Effect of reflow profile on wetting and intermetallic formation between Sn/Ag/Cu solder components and printed circuit boards", *Soldering & Surface Mount Technology*, Vol. 14 No. 2, pp. 18-25.

Bentzen, B. (2000), "Reflow soldering", *SMT in FOCUS*, pp. 1-6, October, available at: www.smtinfocus.com/

Handwerker, C. (2005), "Transitioning to lead-free assemblies", *Printed Circuit Design and Manufacture*, March, pp. 17-23.

Lau, J.H., Wong, C.P., Lee, N.C. and Lee, S.W.R. (2003), *Electronics Manufacturing with Lead-free, Halogen-free & Conductive-adhesive Materials*, Section 15.3, Chapter 15, McGraw-Hill, New York, NY, pp. 15.21-6.

Montgomery, D.C. (1997), *Design and Analysis of Experiments*, 4th ed., Wiley, New York, NY.

Newman, K. (2005), "BGA brittle fracture alternative solder joint integrity test methods", *Proceedings of the 55th IEEE Electronic Components and Technology Conference*,Vol. 2, 31 May-3 June, Lake Buena Vista, FL, pp. 1194-201.

Nurmi, S.T., Sundelin, J.J., Ristolainen, E.O. and Lepisto, T. (2005), "The effect of PCB surface finish on lead-free solder joints", *Soldering & Surface Mount Technology*, Vol. 17 No. 1, pp. 13-23.

Oliver, J.R., Liu, J. and Lai, Z. (2000), "Effect of thermal aging on the shear strength of lead-free solder joints", *Proceedings of the IEEE International Symposium on Advanced Packaging Materials, Braselton, GA, USA*, pp. 152-7.

Rodgers, B., Flood, B., Punch, J. and Waldron, F. (2005), "Determination of the ANAND viscoplasticity model constants for SnAgCu", *Proceedings of the ASME InterPACK conference, San Francisco, CA, USA*, 17-22 July, Paper No. IPACK2005-73352.

Salam, B., Virseda, C., Da, H., Ekere, N.N. and Durairaj, R. (2004), "Reflow profile study of the Sn-Ag-Cu solder", *Soldering & Surface Mount Technology*, Vol. 16 No. 1, pp. 27-34.

Sampathkumar, M., Rajesnayagham, S., Ramkumar, S.M. and Anson, S.J. (2005), "Investigation of the performance of SAC and SACBi lead-free solder alloys with OSP and immersion silver PCB finish", *Proceedings of SMTA International, Chicago, IL, USA*, 25-29 September, pp. 568-75.

Siewert, T., Liu, S., Smith, D.R. and Madeni, J.C. (2002), "Database for solder properties with emphasis on new lead-free solders", NIST & Colorado School of Mines, Release 4.0, available at: www.boulder.nist.gov/div853/lead free/solders.html

Suraski, D. (2000), "The benefits of a ramp-to-spike reflow profile", *SMT*, April, pp. 64-6.

About the authors

Jianbiao Pan, PhD is an Assistant Professor in the Department of Industrial and Manufacturing Engineering at California Polytechnic State University, San Luis Obispo, CA. He received his BE in Mechatronics from Xidian University, Xian, China, in 1990, MS in Manufacturing Engineering from Tsinghua University, Beijing, China, in 1996, a PhD in Industrial Engineering from Lehigh University, Bethlehem, PA, USA in 2000. Prior to joining Cal Poly, he worked at the Optoelectronics Centre of Lucent Technologies/Agere Systems as a member of technical staff. His research interests are in microelectronics packaging, electronics assembly, lead-free soldering, design of experiments, and statistical process control. Dr Pan is a senior member of SME and IMAPS, a member of IEEE and Sigma Xi. He is a recipient of the 2004 M. Eugene Merchant Outstanding Young Manufacturing Engineer Award from SME. Jianbiao Pan is the corresponding author and can be contacted at: pan@calpoly.edu

Brian J. Toleno, PhD is the Application Engineering Team Leader with Henkel in Irvine, California. Brian obtained a PhD in analytical chemistry from Penn State University, and his BS in chemistry from Ursinus College. Prior to working at Henkel Brian managed the failure analysis laboratory at the Electronics Manufacturing Productivity Facility (EMPF).

Brian is an active member of SMTA, served as the Program Chair for the 2005 IEMT, and is active within the IPC serving as the underfill handbook committee (J-STD-030) chairperson and co-chairs the Solder Paste Standards Committee (J-STD-005). Brian has written a course on failure analysis for SMTA and has authored many publications for trade journals and peer reviewed publications, and two chapters for electronic engineering handbooks on adhesives and materials. E-mail: brian.toleno@us.henkel.com

Tzu-Chien Chou received his MS degree in Industrial Engineering from California Polytechnic State University, San Luis Obispo, CA, in 2006. He worked at Solectron's Process technology Group, Milpitas, CA, mainly focusing on RoHS/WEEE activities and lead-free solder joint reliability test in 2005-2006. He is currently an Engineer with IBM Taiwan. E-mail: jason76us@yahoo.com.tw

Wesley J. Dee received his BS in Manufacturing Engineering at California Polytechnic State University, San Luis Obispo, CA, in 2005. He currently works for Maxim Semiconductor as an IC Packaging/Assembly Engineer responsible for new package development and improvements. E-mail: wesleydee01@yahoo.com